Floquet-Engineering Topological Phase Transition in Graphene Nanoribbons by Light

Anhua Huang(黄安华)[1,2], Shasha Ke(柯莎莎)[1,2], Ji-Huan Guan(关济寰)[1,2], Jun Li(李俊)[3], and Wen-Kai Lou(娄文凯)[1,2*]

[1]*SKLSM, Institute of Semiconductors, Chinese Academy of Sciences, Beijing 100083, China*
[2]*College of Materials Science and Opto-electronic Technology, Center of Materials Science and Optoelectronics Engineering, University of Chinese Academy of Sciences, Beijing 100049, China*
[3]*Department of Physics, School of Physical Science and Technology, Xiamen University, Xiamen 361005, China*

(Received 18 June 2024; accepted manuscript online 23 August 2024)

Quasi-one-dimensional (1D) graphene nanoribbons (GNRs) play a crucial role in advancement of next-generation devices. Recent studies have suggested their potential to exhibit unique symmetry-protected topological phases defined by a Z_2 invariant. By employing both the tight-binding model and the Floquet theory, our investigation demonstrates the effective control of the topological phase within quasi-1D armchair GNRs (AGNRs) using elliptically polarized light, unveiling rich topological phase diagrams. Specifically, we observe that varying the amplitude of the light can induce transitions in the band gap (E_g) of AGNRs, leading to multiple changes in the system's Z_2 invariant. Furthermore, for heterojunctions composed of different AGNR segments, the junction state can be either created or eliminated by the application of elliptically polarized light.

DOI: 10.1088/0256-307X/41/9/097302

Topological insulators have been a subject of considerable interest due to their distinct characteristics, featuring a gapped spectrum in the bulk and metallic edge states that remain robust against perturbations.[1–9] While the majority of these reports have concentrated on two-dimensional or three-dimensional (2D/3D)[1–9] topological insulators, investigating into the mechanism driving the transition between these dimensional phases, lately there has been significant interest in quasi-one-dimensional (1D) systems such as graphene nanoribbons (GNRs) due to special electronic structures[10,11] and potential to exhibit unique symmetry-protected topological phases.[12–22] A wealth of research has explored the topological classification of different GNRs defined by the Z_2 invariant.[12,14,22,23] The Z_2 invariants associated to these GNRs exhibit sensitivity to factors such as their width, symmetry, and geometric boundaries. Significantly, the existence of topological junction states in heterojunctions created by alternating segments of GNRs has been verified by both theoretical analyses[12,14] and experimental studies.[16]

Effectively and precisely manipulating the topological phases of materials represents a critical realm of investigation, bearing implications for both fundamental physics and the practical utilization of topological insulators. In 2D/3D systems, extensive studies have investigated topological phase transitions using various methods.[24–29] However, the strategies for tuning topological phases of 1D systems have been relatively limited, primarily involving techniques such as the incorporation of boron-nitrogen atoms, application of external transverse electric fields,[21] and our previous work involving external strain.[30] Generally, strain can alter the electronic structures of the honeycomb lattice, resulting in intriguing phenomena like the pseudomagnetic field[31–34] and Goos–Hänchen.[35] However, both of the two methods are complicated and painful, which may cause irrecoverable destructive effects on the lattice or rely on very precise strain design. These disadvantages hinder the practical application possibility of 1D topological GNRs.

This study presents a novel method for inducing topological phase transitions in 1D armchair GNRs (AGNRs) with rich topological phase diagrams using elliptically polarized light. The AGNRs undergo a topological phase transition with a variation in the Z_2 invariant sensitively depending on the width of the AGNRs. By increasing the intensity of the light, multiple topological phase transitions can be induced. Notably, the junction states in heterojunctions composed of AGNRs with differing topological properties can be either created or eliminated by the application of the light. This study presents a user-friendly and straightforward method for manipulating topological phase transitions in quasi-1D materials, providing an efficient approach to control junction states.

The tight-binding (TB) model of AGNRs can be expressed as

$$H = \sum_i \epsilon_i a_i^\dagger a_i - \sum_{\langle ij \rangle} t a_i^\dagger a_j + \text{H.c.}, \tag{1}$$

where $a_i^\dagger$ and a_i denote the creation and annihilation operators. Respectively, the parameter ϵ_i is the onsite energy and t represents the hopping energy. We utilize the

*Corresponding author. Email: wklou@semi.ac.cn
© 2024 Chinese Physical Society and IOP Publishing Ltd

Pybinding[36] and PythTB[37] packages to extract electronic structures and investigate the topological properties of the systems.

The Zak phase, which signifies Berry's phase[12,30,38] acquired by a particle traversing the Brillouin zone (BZ), plays a pivotal role in characterizing the topological phases in quasi-1D systems. It can be obtained by integrating the Berry connection $i\langle\varphi_{nk}|\nabla_k\varphi_{nk}\rangle$ as follows:

$$\gamma_n = i(2\pi/L)\int_{-\pi/L}^{\pi/L} dk\langle\varphi_{nk}|\nabla_k\varphi_{nk}\rangle, \tag{2}$$

where k represents the wave vector, L the size of the unit cell, and φ_{nk} the periodic component of the Bloch wave function of band n. The Zak phase could be expressed in two components as follows:[12,15,30,39]

$$\gamma_n = \gamma_{1,n} + \gamma_{2,n}. \tag{3}$$

For the systems exhibiting spatial symmetries, the $\gamma_{1,n}$ makes no contribution to the Zak phase.[12] A quantized Zak phase of a band assumes a value of either 0 or π, corresponding to a topologically trivial or nontrivial band, respectively.[12,30,38]

The topological phase of AGNRs can be characterized by the Z_2 invariant[4] calculated as the sum of the Zak phase of all the occupied bands, i.e.,[12]

$$(-1)^{Z_2} = e^{i\sum_n \gamma_n}. \tag{4}$$

For the AGNRs, the $Z_2 = 0(1)$ represents a topological trivial (nontrivial) phase.

Here we study the control of topological states by light fields. We choose an elliptically polarized light[40] with a vector potential $\boldsymbol{A}$ of the form:

$$\boldsymbol{A}(\tau) = (A_x\sin(\Omega\tau), A_y\sin(\Omega\tau+\phi_0)), \tag{5}$$

where ϕ_0 is the phase difference between the x and y components. This vector potential gives a time-dependent electric field $\boldsymbol{E}(\tau) = -\partial\boldsymbol{A}/\partial\tau = -(A_x\Omega\cos(\Omega\tau), A_y\Omega\cos(\Omega\tau+\phi_0))$. The effect of the elliptically polarized light is incorporated into the Hamiltonian through Peierls substitution,[41] where the hopping parameter with a time-dependent Peierls phase is given by

$$t(\tau) = t\exp[-i\frac{e}{\hbar}\boldsymbol{A}(\tau).(\boldsymbol{r}_i - \boldsymbol{r}_j)], \tag{6}$$

The time-dependent Hamiltonian can be solved numerically within the framework of Floquet theory.[42–44] The optically driven systems are described by the time-dependent Schrödinger equation

$$i\hbar\frac{\partial}{\partial\tau}\Psi(\tau) = H(\tau)\Psi(\tau). \tag{7}$$

The Hamiltonian $H(\tau)$ is time-periodic with $H(\tau) = H(\tau+T)$ for a period $T = 2\pi/\Omega$ of elliptically polarized light. According to the Floquet theory, the wavefunction $\Psi(\tau)$ can be written as

$$\Psi(\tau) = e^{-iE\tau/\hbar}\Phi(\tau), \tag{8}$$

where $\Phi(\tau)$ and E represent the Floquet state and the quasi-energy. We substitute Eq. (8) into Eq. (7) and perform a Fourier transformation. The time-dependent Schrödinger equation is rewritten as

$$\sum_{n=-\infty}^{\infty}(H_{mn} - n\Omega\delta_{m,n})\Phi_\mu^n = E_\mu^m\Phi_\mu^m. \tag{9}$$

Here, the Fourier coefficients H_{mn} and Φ_μ^m can be written as

$$H_{mn} = \frac{1}{T}\int_0^T e^{i(m-n)\Omega\tau}H(\tau)d\tau, \tag{10}$$

$$\Phi_\mu^m = \frac{1}{T}\int_0^T e^{im\Omega\tau}\Phi_\mu(\tau)d\tau, \tag{11}$$

where n, m are the Floquet replica numbers. After the Peierls substitution, the H_{mn} can be written as

$$H_{mn} = \frac{1}{T}\int_0^T e^{i(m-n)\Omega\tau}\exp[-i\frac{e}{\hbar}\boldsymbol{A}(\tau).(\boldsymbol{r}_i - \boldsymbol{r}_j)]d\tau. \tag{12}$$

The electronic structures of AGNRs can be classified into three distinct groups based on E_g exhibiting highly sensitivity to the width (N) of the systems. These classifications are commonly denoted as $N = 3q$, $N = 3q+1$, and $N = 3q+2$, where q is an integer. In the subsequent discourse, we will explore the scenario where $N = 3q$ for simplicity. However, discussions pertaining to $N = 3q+2$ and $N = 3q+1$ can be found in the Supplemental Material.

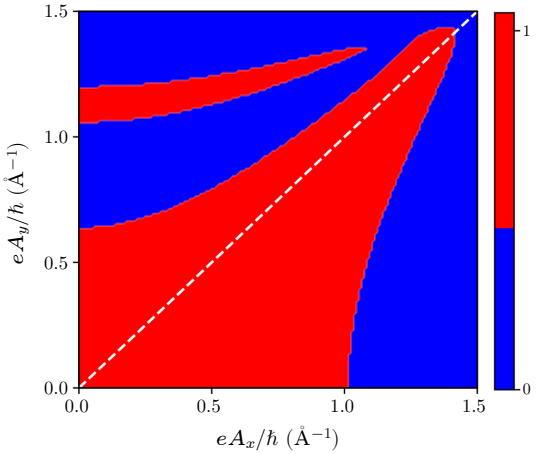

Fig. 1. The Z_2 invariant as a function of drive amplitudes A_x and A_y with phase $\phi_0 = \pi/2$ of elliptically polarized light for AGNR ($N = 9$). We have used $\hbar\Omega = 10$ eV, which is much larger than the band gap. The white dashed line represents circularly polarized light.

Figure 1 shows the rich topological phase diagram of AGNR $N = 9$ as a function of the drive amplitudes with $\phi_0 = \pi/2$, for a fixed frequency $\hbar\Omega = 10$ eV, which is much greater than the band gap and is in the off-resonant case. Such an energy of light could be achieved in the experiment.[45,46] The red (blue) color represents $Z_2 = 1$ ($Z_2 = 0$). We find that there is no symmetry about the $A_x = A_y$ (as shown by the white dashed line in Fig. 1) which indicates that the topological properties are anisotropic with the response of circularly polarized light. The on-resonant case with lower energy for $\hbar\Omega = 4$ eV and $\hbar\Omega = 5$ eV are shown in Fig. S1 in the Supplementary Material for $N = 9$. In the phase diagram, we can also

find topological phase transition with lower energy pump light. We also calculate the different ϕ_0 in the Supplementary Material for $N = 9$, $N = 11$, and $N = 13$. We can find that if the phase has the relationship $\phi_0 = -\phi_0$ or $\phi_0 = \pi - \phi_0$, we can get the same phase diagram.

The band structures for the AGNR ($N = 9$) under the elliptically polarized light with $A_y = 4A_x$ are shown in Figs. 2(a)–2(c). In the equilibrium state (without light), a finite E_g is observed [Fig. 2(a)], with the Z_2 invariant equal to 1, signifying that the system is in a topologically nontrivial phase in the absence of light.

Remarkably, the E_g can be efficiently regulated through the application of the light [Fig. 2(b) and 2(c)]. At a critical amplitude of $eA_x/\hbar = 0.164\,\text{Å}^{-1}$, the E_g closes, leading to the emergence of a gapless Dirac cone [Fig. 2(b)]. The Z_2 invariant of this semimetallic phase could not be calculated. Upon further increasing the amplitude, such as by raising $eA_x/\hbar$ to $0.25\,\text{Å}^{-1}$ [Fig. 2(c)], the E_g reopens and the Z_2 invariant is 0. This phenomenon suggests that the system transitions from a topological phase to a normal insulator phase, driven by the elliptically polarized light.

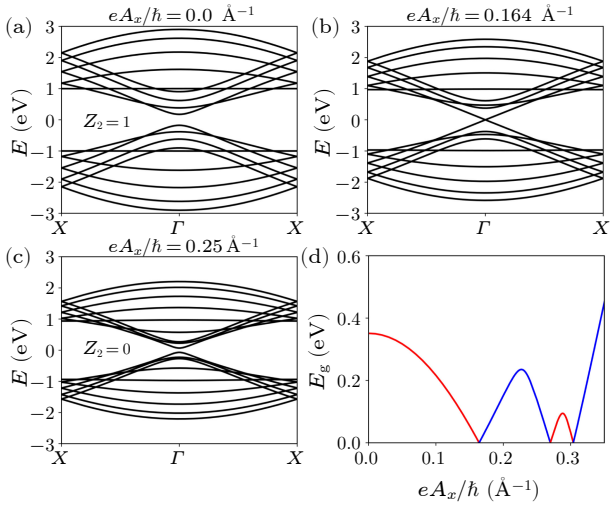

Fig. 2. Band structure and band gap of the AGNR ($N = 9$) under the elliptically polarized light with $A_y = 4A_x$: (a) for $eA_x/\hbar = 0.0\,\text{Å}^{-1}$, (b) for $eA_x/\hbar = 0.164\,\text{Å}^{-1}$, (c) for $eA_x/\hbar = 0.25\,\text{Å}^{-1}$. (d) The band gap as a function of $eA_x/\hbar$. The Z_2 invariants are listed. The blue (red) color indicates $Z_2 = 0$ ($Z_2 = 1$).

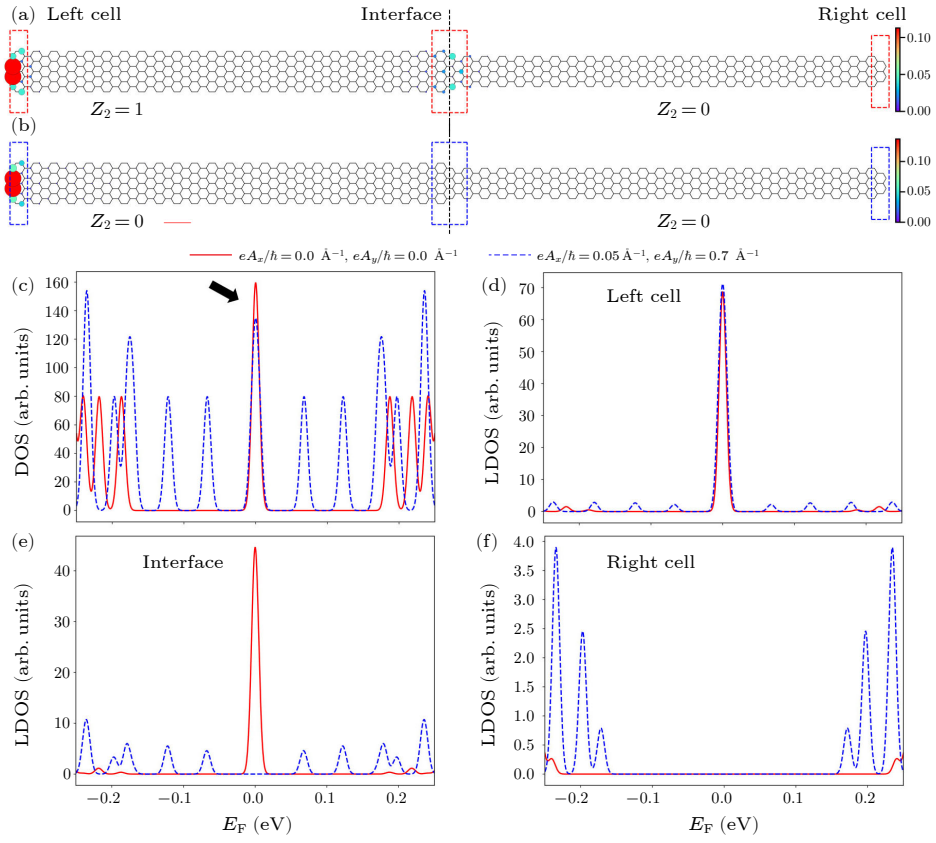

Fig. 3. The heterojunction comprised of finite AGNR segments with $N = 9$ and $N = 7$ AGNRs (9AGNR/7AGNR), consisting of 25 unit cells for everyone. The heterojunction is illustrated in (a) without elliptically polarized light and (b) with elliptically polarized light, respectively. The charge density distribution is illustrated by colored and differently sized balls, representing the intensity of the charge distribution. (c) The density of states (DOS) for the heterojunction, both with and without the influence of elliptically polarized light. The charge density distribution is calculated at the energy labeled by the arrow. (d)–(f) The LDOS of the heterojunction for left cell of 9AGNR, interface and right cell of 7AGNR with and without elliptically polarized light. The left cell, interface and right cell are labeled in (a) and (b). The Z_2 invariants for the two segments of the heterojunction are depicted in panels (a) and (b).

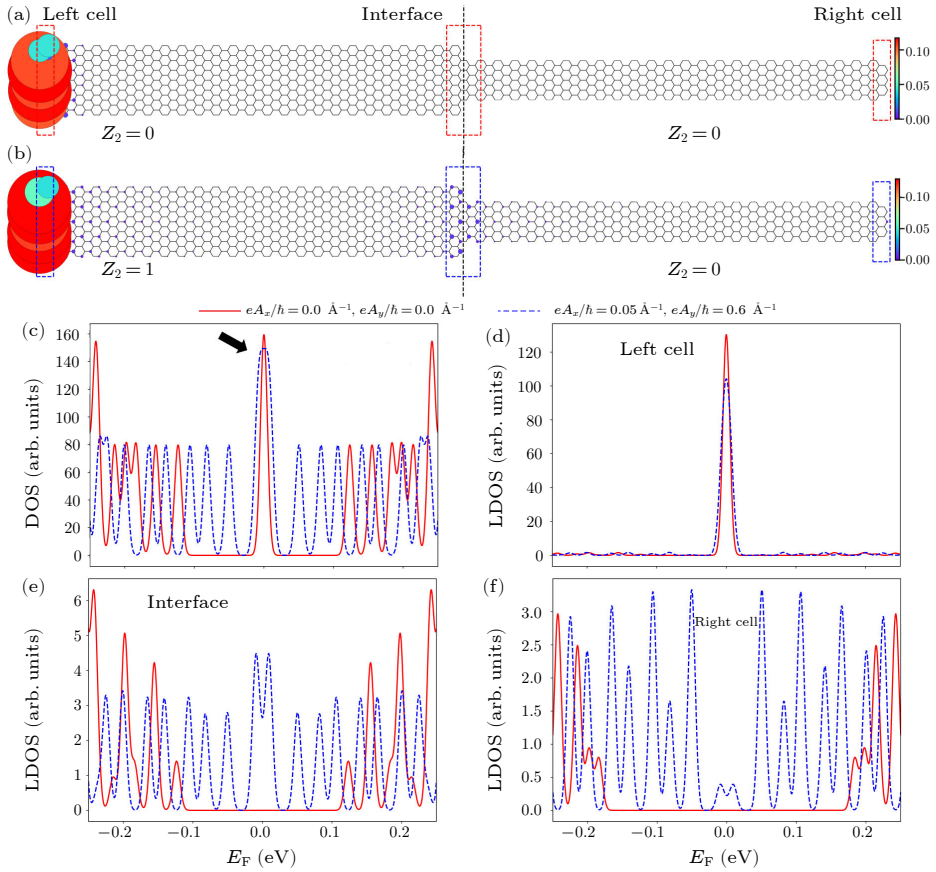

Fig. 4. The heterojunction comprised of finite AGNR segments with $N = 15$ and $N = 9$ AGNRs (15AGNR/9AGNR), consisting of 25 unit cells for everyone. The heterojunction is illustrated in (a) without elliptically polarized light and (b) with elliptically polarized light, respectively. The charge density distribution is illustrated by colored and differently sized balls, representing the intensity of the charge distribution. (c) The density of states (DOS) for the heterojunction, both with and without the influence of elliptically polarized light. The charge density distribution is calculated at the energy labeled by the arrow. (d)–(f) The LDOS of the heterojunction for left cell of 15AGNR, interface and right cell of 9AGNR with and without elliptically polarized light. The left cell, interface and right cell are labeled in (a) and (b). The Z_2 invariants for the two segments of the heterojunction are depicted in panels (a) and (b).

Figure 2(d) shows the E_g as a function of the amplitude A_x, providing a broader perspective on the impact of light on the topological properties of the system. In the range from $eA_x/\hbar = 0.0\,\text{Å}^{-1}$ to $eA_x/\hbar = 0.35\,\text{Å}^{-1}$, the E_g becomes 0 several times with multiple changes of topological invariant, indicating that multiple topological phase transitions can occur under the elliptically polarized light. However, it is crucial to note that the initial topological state of the AGNRs significantly influences the subsequent topological phase transitions.

In such unique 1D topological materials, there are a junction state (JS) and end states (ESs) in the AGNR heterojunctions with finite AGNR segments originating from the topological properties of the electronic structure of their components. The capability to control the ESs and JS of heterojunctions holds promise for potential applications. However, how to achieve precise manipulation of the topological phases, JS and ESs, in 1D systems continues to present a significant challenge. In the above discussion, we have realized that elliptically polarized light can be well tuned to topological phase of the AGNRs. Next, we explore how the elliptically polarized light impacts the ESs and JS in heterojunctions. Guiding by the Z_2 invariants across different widths, we establish a heterojunction of AGNRs, comprising a 9AGNR ($N = 9$) and a 7AGNR ($N = 7$) with a zigzag' end termination.[12] This heterojunction, named as 9AGNR/7AGNR, consists of 25 unit cells for each segment as shown in Figs. 3(a) and 3(b). In the equilibrium case, the presence of the JS and ESs of the 9AGNR/7AGNR heterojunction has been experimentally verified.[16]

In the equilibrium case, we calculate the Z_2 invariants for the 9AGNR and 7AGNR as 1 and 0, respectively, as indicated in Fig. 3(a). When applying the elliptically polarized light with $eA_x/\hbar = 0.05\,\text{Å}^{-1}$ and $eA_y/\hbar = 0.7\,\text{Å}^{-1}$, based on Eq. (4), we can get that the 9AGNR and 7AGNR segments have the same Z_2 invariant with $Z_2 = 0$, as indicated in Fig. 3(b). The density of states (DOS) of the heterojunction is illustrated in Fig. 3(c), where the blue dashed line (red solid line) represents the absence (presence) of light.

We find sharp peaks at $E_F = 0\,\text{eV}$ in the DOS, no matter whether or not the influence of light is applied. The peak at $E_F = 0\,\text{eV}$ without light is slightly

higher than the situation with light, which is different from the strain field.[30] In previous studies, there is no such a shark peak in the DOS for the heterojunction constituted by topologically equivalent AGNRs.[12,14] However, with proper amplitude of light for $eA_x/\hbar = 0.05\,\text{Å}^{-1}$ and $eA_y/\hbar = 0.7\,\text{Å}^{-1}$, we still find such sharp peaks at $E_\text{F} = 0\,\text{eV}$, which is in sharp contrast of previous report. To further validate the states at $E_\text{F} = 0\,\text{eV}$ with and without light, we plot the charge density distribution for this heterojunction, as shown in Figs. 3(a) and 3(b) with different colors and sizes of the balls. We find that: (1) In the absence of light, the states at $E_\text{F} = 0\,\text{eV}$ are composed of both JS at the interface of the heterojunction and ESs at the edge of the 9AGNR. (2) In the presence of light, the states are only composed of ESs at the edge of the 9AGNR. In other words, no matter whether or not the influence of light exists, ESs are remained at the edge of the 9AGNR, while the existence of JS sensitively depends on the amplitude of the light. We can draw a conclusion that the JS of the heterojunction can be eliminated by the application of light.

The fundamental physics driving such a phenomenon is quite simple. When light is introduced to the system, the AGNRs of the heterojunction transition from being topologically inequivalent to becoming topologically equivalent, leading to the elimination of the JS. To further validate our conclusions, the local densities of states (LDOSs) for the left cell of the 9AGNR, the interface, and the right cell of the 7AGNR are calculated, as shown in Figs. 3(d)–3(f). Regardless of the light, as shown in Fig. 3(d), the LDOSs of left cell exhibit a sharp peak at $E_\text{F} = 0\,\text{eV}$. The peak for the heterojunction in the presence of light (blue dashed line) is slightly larger than the situation in the absence of light (red solid line), indicating that the light could make the charge at the interface to move to the edge. As shown in Fig. 3(e), a distinct peak at $E_\text{F} = 0\,\text{eV}$ is solely evident at the interface of the heterojunction in the absence of light caused by the presence of JS, indicating that the JS can be eliminated by the application of light. Moreover, as shown in Fig. 3(f), there is no peak at $E_\text{F} = 0\,\text{eV}$ for the right cell, regardless of the light, suggesting the lack of ESs in the edge of 7AGNR which can be ascribed to the quantum confinement effect.

Additionally, we explore the 15AGNR/9AGNR heterojunction, where the Z_2 invariant is 0 for both the 15AGNR and 9AGNR in the absence of light, as shown in Fig. 4(a). However, when light with $eA_x/\hbar = 0.05\,\text{Å}^{-1}$ and $eA_y/\hbar = 0.6\,\text{Å}^{-1}$ is applied, the Z_2 invariant for 15AGNR changes to 1 and the Z_2 invariant for 9AGNR keeps unchanged, as shown in Fig. 4(b). Remarkably, we find that JS can be created by the application of light, as shown in Figs. 4(b)–4(f). Therefore, the elliptically polarized light possesses the capability to either create or eliminate JS. This suggests that by the application of elliptically polarized light, we can effectively manipulate and regulate the characteristics of the JS within the heterojunction.

In summary, we have presented an innovative and reversible method for designing 1D AGNRs with customizable topological phases by utilizing elliptically polarized light. This transition occurs by closing and reopening the band gap, thereby changing the Z_2 invariant of the system from 1 to 0, or vice versa, effectively inducing the topological phase transition. With the increase of the amplitude of elliptically polarized light, the multiple topological phase transitions can occur with rich topological phase diagrams. Moreover, we introduce a novel strategy for manipulating the junction state in heterojunctions composed of diverse topological segments of AGNRs through the application of elliptically polarized light. By tuning the amplitude of elliptically polarized light, we can create or eliminate the junction state within the heterojunction. Our study presents a promising approach for fine-tuning topological phase transitions in flexible quasi-1D materials, enabling control and customization of the properties of the junction state in a convenient, non-invasive, and reversible manner.

Acknowledgements. This work was supported by the National Natural Science Foundation of China (Grant Nos. 92265203 and 11974340), the Strategic Priority Research Program of the Chinese Academy of Sciences (Grants Nos. XDB0460000, XDB28000000, and XDPB22), the Innovation Program for Quantum Science and Technology (Grant No. 2024ZD0300104), and the National Key Research and Development Program of China (Grant No. 2018YFA0306101).

References

[1] Kane C L and Mele E J 2005 *Phys. Rev. Lett.* **95** 226801
[2] Bernevig B A and Zhang S C 2006 *Phys. Rev. Lett.* **96** 106802
[3] Bernevig B A, Hughes T L, and Zhang S C 2006 *Science* **314** 1757
[4] Fu L and Kane C L 2007 *Phys. Rev. B* **76** 045302
[5] Konig M, Wiedmann S, Brune C, Roth A, Buhmann H, Molenkamp L W, Qi X L, and Zhang S C 2007 *Science* **318** 766
[6] Hasan M Z and Kane C L 2010 *Rev. Mod. Phys.* **82** 3045
[7] Qian X, Liu J, Fu L, and Li J 2014 *Science* **346** 1344
[8] Fu L, Kane C L, and Mele E J 2007 *Phys. Rev. Lett.* **98** 106803
[9] Zhang H, Liu C X, Qi X L, Dai X, Fang Z, and Zhang S C 2009 *Nat. Phys.* **5** 438
[10] Fujita M, Wakabayashi K, Nakada K, and Kusakabe K 1996 *J. Phys. Soc. Jpn.* **65** 1920
[11] Son Y W, Cohen M L, and Louie S G 2006 *Phys. Rev. Lett.* **97** 216803
[12] Cao T, Zhao F, and Louie S G 2017 *Phys. Rev. Lett.* **119** 076401
[13] Gröning O, Wang S Y, Yao X L, Pignedoli C A, Borin Barin G, Daniels C, Cupo A, Meunier V, Feng X L, Narita A, Müllen K, Ruffieux P, and Fasel R 2018 *Nature* **560** 209
[14] Lee Y L, Zhao F, Cao T, Ihm J, and Louie S G 2018 *Nano Lett.* **18** 7247
[15] Lin K S and Chou M Y 2018 *Nano Lett.* **18** 7254
[16] Rizzo D J, Veber G, Cao T, Bronner C, Chen T, Zhao F, Rodriguez H, Louie S G, Crommie M F, and Fischer F R 2018 *Nature* **560** 204
[17] Joost J P, Jauho A P, and Bonitz M 2019 *Nano Lett.* **19** 9045
[18] Jiang J and Louie S G 2021 *Nano Lett.* **21** 197
[19] Liu D X, Li X F, Zhang X H, Cao X, Zhu X J, and Shi D 2020 *J. Phys. Chem. C* **124** 15448
[20] Sun Q, Yan Y Y, Yao X L, Müllen K, Narita A, Fasel R, and Ruffieux P 2021 *J. Phys. Chem. Lett.* **12** 8679
[21] Zhao F, Cao T, and Louie S G 2021 *Phys. Rev. Lett.* **127** 166401

[22] Arnold F M, Liu T J, Kuc A, and Heine T 2022 *Phys. Rev. Lett.* **129** 216401
[23] Li J, Sanz S, Merino-Díez N, Vilas-Varela M, Garcia-Lekue A, Corso M, de Oteyza D G, Frederiksen T, Peña D, and Pascual J I 2021 *Nat. Commun.* **12** 5538
[24] Li J and Chang K 2009 *Appl. Phys. Lett.* **95** 222110
[25] Miao M S, Yan Q, Van de Walle C G, Lou W K, Li L L, and Chang K 2012 *Phys. Rev. Lett.* **109** 186803
[26] Zhang D, Lou W, Miao M, Zhang S C, and Chang K 2013 *Phys. Rev. Lett.* **111** 156402
[27] Liu J and Vanderbilt D 2013 *Phys. Rev. B* **88** 224202
[28] Antonius G and Louie S G 2016 *Phys. Rev. Lett.* **117** 246401
[29] Monserrat B and Vanderbilt D 2016 *Phys. Rev. Lett.* **117** 226801
[30] Huang A, Ke S, Guan J H, Li J, and Lou W K 2024 *Phys. Rev. B* **109** 045408
[31] Zhang D B, Seifert G, and Chang K 2014 *Phys. Rev. Lett.* **112** 096805
[32] Li Y M, Zhou X, Zhang Y Y, Zhang D, and Chang K 2017 *Phys. Rev. B* **96** 035406
[33] Ke S, Li Y M, Lou W K, and Chang K 2023 *Phys. Rev. B* **107** 104426
[34] Wei B, Zhu J J, Song Y, and Chang K 2024 *Phys. Rev. Res.* **6** 013210
[35] Wu Z, Zhai F, Peeters F M, Xu H Q, and Chang K 2011 *Phys. Rev. Lett.* **106** 176802
[36] Moldovan D, Andelkovic M, and Peeters F 2020 Pybinding v0.9.5: A Python package for Tight-Binding Calculations
[37] Coh S and Vanderbilt D 2016 Python Tight Binding (PythTB) v1.7.2
[38] Zak J 1989 *Phys. Rev. Lett.* **62** 2747
[39] Rhim J W, Behrends J, and Bardarson J H 2017 *Phys. Rev. B* **95** 035421
[40] Seshadri R and Sen D 2022 *Phys. Rev. B* **106** 245401
[41] Peierls R 1933 *Z. Phys.* **80** 763
[42] Zhu H X, Wang T T, Gao J S, Li S, Sun Y J, and Liu G L 2014 *Chin Phys. Lett.* **31** 030503
[43] Rudner M S and Lindner N H 2020 arXiv:2003.08252 [cond-mat.mes-hall]
[44] Lei L X, Wang W C, Huang G Y, Hu S, Cao X, Zhang X F, Deng M T, and Chen P X 2024 *Chin. Phys. Lett.* **9** 090301
[45] Berntsen M H, Götberg O, and Tjernberg O 2011 *Rev. Sci. Instrum.* **82** 095113
[46] He Y, Vishik I M, Yi M, Yang S, Liu Z, Lee J J, Chen S, Rebec S N, Leuenberger D, Zong A, Jefferson C M, Moore R G, Kirchmann P S, Merriam A J, and Shen Z X 2016 *Rev. Sci. Instrum.* **87** 011301